Biochemistry and Biophysics Reports 8 (2016) 340–345

Contents lists available at ScienceDirect

Biochemistry and Biophysics Reports

journal homepage: www.elsevier.com/locate/bbrep

Role of MIZ-1 in *AMELX* gene expression

Hee-Jin Noh[a,1], Dong-In Koh[a,1], Kon-O. Lee[b], Bu-Nam Jeon[a], Min-Kyeong Kim[a], Malcom L. Snead[c], Man-Wook Hur[a,*]

[a] *Brain Korea 21 Plus Project for Medical Science, Department of Biochemistry and Molecular Biology, Severance Biomedical Research Institute, Yonsei University School of Medicine, 134 ShinChon-Dong, SeoDaeMoon-Ku, Seoul 120-752, Korea*
[b] *Kanagawa Dental University, 82 Inaooka-Chou, Yokosuka-Shikanagawa-Ken, Japan*
[c] *The Center for Craniofacial Molecular Biology, The Herman Ostrow School of Dentistry of the University of Southern California, Los Angeles, CA, USA*

ARTICLE INFO

Keywords:
MIZ-1
Amelx
Odontoblast differentiation
Odontoblast mineralization

ABSTRACT

Amelogenin (AMELX) is the main component of the developing tooth enamel matrix and is essential for enamel thickness and structure. However, little is known about its transcriptional regulation. Using gene expression analysis, we found that MIZ-1, a potent transcriptional activator of *CDKN1A*, is expressed during odontoblastic differentiation of hDPSCs (human dental pulp stem cells), and is essential for odontoblast differentiation and mineralization. We also investigated how MIZ-1 regulates gene expression of *AMELX*. Oligonucleotide-pull down assays showed that MIZ-1 binds to an MRE (MIZ-1 binding element) of the *AMELX* proximal promoter region (bp, −170 to −25). Combined, our ChIP, transient transcription assays, and promoter mutagenesis revealed that MIZ-1 directly binds to the MRE of the *Amelx* promoter recruits p300 and induces *Amelx* gene transcription. Finally, we show that the zinc finger protein MIZ-1 is an essential transcriptional activator of *Amelx*, which is critical in odontogenesis and matrix mineralization in the developing tooth.

1. Introduction

Tooth development is controlled by extensive “crosstalk” between epithelium and mesenchyme, involving ligand–receptor interactions that induce transcriptiomic changes that orchestrate cellular processes required for tooth development [1]. During tooth formation, the ectoderm thickens and forms a placode that buds into the underlying neural-crest derived mesenchyme. The epithelium then signals to the mesenchyme, resulting in condensation around the epithelial bud [2–5]. After the bud stage, the epithelium starts to extend further into the mesenchyme, wrapping around the condensing mesenchyme via structures created at its center, known as “primary enamel knots,” that instruct the patterning of the tooth crown and regulate the location and height of tooth cups [2–5]. Cervical loops fold around the condensing mesenchyme. At the late-cap to early-bell stages, high levels of apoptosis occur within the enamel knot, leading to the eventual loss of the structure and silencing of the signaling center. During the bell stages, cytodifferentiation occurs, in which the adjacent layer of epithelial cells differentiates into ameloblasts that secrete the enamel matrix, while the mesenchyme differentiates into odontoblasts, producing dentin [2–5].

Ameloblasts secrete the enamel-forming amelogenin family of proteins, which play a key role in regulating proper tooth enamel and replacement, by the mineral phase, generating a “woven” architecture [6]. Dental enamel is the hardest tissue in the body and cannot be replaced or repaired, because ameloblasts are lost at tooth eruption. Amelogenin proteins constitute 90% of the extracellular matrix secreted by ameloblasts, and these proteins are cleaved in a regulated process during enamel maturation [7,8]. Several mutations in the human X-chromosomal *AMELOGENIN* (*AMELX*) gene have been reported that lead to X-linked amelogenesis imperfecta 1 (AI 1) [9], an inherited enamel defect characterized by phenotypic variability, in which patients present with hypoplastic defects (“thin-pitted” or “grooved” enamel) and/or hypomineralization, where the enamel mineral content is decreased [7].

Amelogenin expression is and developmentally regulated at the temporal and spatial levels [10–14], at both the transcriptional and post-transcriptional levels [1]. Moreover, using transgenic mouse analysis, a 2263-nucleotide promoter element from the mouse X-chromosomal *Amelx* gene was demonstrated to recapitulate the spatiotemporal expression pattern of the endogenous *Amelx* gene [13]. Homologies (70% identity) in the 300-nucleotide region upstream of the transcription initiation site exist between the murine, bovine, and human X-chromosomal amelogenin gene, suggesting that this

* Correspondence to: Department of Biochemistry and Molecular Biology, Yonsei University School of Medicine, 134, ShinChon-Dong, SeoDaeMoon-Ku, Seoul 120-752, Korea.
E-mail address: mwhur2@yuhs.ac (M.-W. Hur).
[1] The two fist authors contributed equally.

http://dx.doi.org/10.1016/j.bbrep.2016.10.007
Received 14 June 2016; Received in revised form 13 September 2016; Accepted 9 October 2016
Available online 15 October 2016

region is likely long conserved for transcription of this important gene (*Amelx*).

Several transcription factors have been shown to regulate *Amelx*. Its promoter region contains a reversed CCAAT box four base pairs downstream from the C/EBPα-binding site. CCAAT/enhancer-binding protein α (C/EBPα) plays a strong role in developmental control of *Amelx*, , while the tooth development regulator Msx2 interferes with C/EBPα binding at the mouse *Amelx* minimal promoter by protein-protein interaction [15]. Moreover, NF-Y synergistically acts with C/EBPα to activate mouse *Amelx* during amelogenesis [16], while the tooth germ proteins Foxj1 and Dlx2 function independently to activate the *Amelx* promoter [17].

MIZ-1 is a member of the POK family proteins, BTB/POZ domain protein having one or more Krüppel-like zinc-fingers [18]. Previous reports showed that MIZ-1 is a potent transcriptional activator of *CDKN1A* [18], and it interacts with various oncoproteins, such as c-MYC, BCL6, ZBTB4 and GFI-1, to transcriptionally repress genes involved in cellular differentiation and metabolism [18–20]. More recently, POK family proteins have also been characterized as transcriptional regulators of genes that control cell proliferation [21]. Although POK family proteins appear to play key roles in various cellular regulatory process, functions of many POK family proteins remain largely unknown [21].

Here, we found that MIZ-1 is expressed in hDPSCs (human dental pulp stem cells) during odontoblastic differentiation, and is temporally regulated during odontoblastic differentiation of hDPSCs. MIZ-1 modulates *AMELX* expression and thus, odontoblastic differentiation.

2. Materials and methods

2.1. Cell culture and transient transfection assays

Human embryonic kidney (HEK293) and dental pulp stem cells (hDPSCs, CEFO Research Center, Seoul, Korea), and murine embryonic fibroblasts (MEFs) and LS8 ameloblast-like cells were cultured in Dulbecco's Modified Eagle's Medium (DMEM, Gibco-BRL, Grand Island, NY, USA), supplemented with 10% fetal bovine serum (FBS, Hyclone, Logan, UT, USA), 100 μg/ml streptomycin, and 100 units/ml penicillin, at 37 °C in a humidified, 5% CO_2 incubator. To induce odontoblast differentiation, hDPSCs were cultured in DMEM supplemented with 10% FBS, a P/S (penicillin/streptomycin) solution, 50 mg/ml ascorbic acid, 10 mmol/l sodium β-glycerol phosphate, and 10 nmol/l dexamethasone.

Various combinations of the plasmids pGL2-*Amelx*-Luc −485 bp, pGL2-*Amelx*-Luc −70 bp, pcDNA3.1, and pcDNA3.1-MIZ-1 were transiently transfected into murine LS8 cells using Lipofectamine Plus reagent (Invitrogen, Carlsbad, CA, USA), cultured for 24–36 h, and analyzed for luciferase activity, using a Microplate LB 96V luminometer (EG & G Berthold, Wildbad, Germany). All reactions were performed in triplicate and presented as means ± SDs. Reporter activity was normalized to coexpressed β-galactosidase activity, or total cellular protein.

2.2. Electroporation

Electroporation was performed using a Neon Transfection System (Invitrogen), according to the manufacturer's instructions. MEF cells were washed with PBS, resuspended in electroporation buffer containing plasmid DNA, and electroporated (1350 V, pulse width 30 ms, pulse number 1), using a 100 μl tip. After electroporation, cells were cultured in DMEM medium and allowed to recover for 72 h.

2.3. Odontoblastic differentiation of hDSPPs and alizarin red staining

hDSPPs were cultured in odontoblastic induction medium for 14 days, and mineralization was assessed at 0, 7, and 14 days by staining with Alizarin red (Sigma-Aldrich, St-Louis, MO, USA). The cells were grown in 10 cm dishes, fixed with 1 ml 10% formaldehyde for several minutes at room temperature, washed with distilled water, and stained with 1% alizarin red (pH 5.5) for 30 min at room temperature.

2.4. Total RNA isolation and RT-PCR

Total RNA was isolated from cells using TRIzol reagent (Invitrogen). cDNA was synthesized using 2 μg of total RNA, random hexamers (10 pmol), oligo-dT (10 pmol), and Superscript reverse transcriptase II (200 units), in a total volume of 20 μl, using a reverse transcription kit (Invitrogen). PCR was then performed using the following cycling conditions: 94 °C denaturation for 3 min, followed by 25, 30, 35, or 40 cycles of amplification (94 °C for 30 s, 55 °C for 30 s, 72 °C for 30 s), and a final extension at 72 °C for 5 min. The following oligonucleotide PCR primers were:

MIZ-1 forward, 5′-CAGCCGTCACTCAGCTCA-3′, reverse, 5′-ATCAGCAAAGCTGTGAAGCAAGT-3′; *GAPDH* forward, 5′-ACCACAGTCCATGCCATCAC-3′, reverse, 5′-TCCACCACCCTGTTGCTGTA-3′; *AMELX* forward, 5′-TCCCCCAGCAACCAATGAT-3′, reverse, 5′- GAACATCGGAGGCAGAGGTG-3′; *DMP-1* forward, 5′-ACAGGCAAATGAAGACCC-3′, reverse, 5′-TTCACTGGCTTGTATGG-3′.

2.5. Quantitative real-time PCR (qRT-PCR) analysis

Quantitative qRT-PCR reactions were conducted with SYBR Green PCR Master Mix, using an ABI PRISM 7300 RT-PCR System (Applied Biosystems, Foster City, CA, USA). All reactions were performed in triplicate; 18S ribosomal RNA was used as a control. The following oligonucleotides were used as PCR primers:

Amelx forward, 5′-CCCCTGTCCCCCATTCTT-3′, reverse, 5′-TCCCGCTTGGTCTTGTCTGT-3′; *18S* forward, 5′-CCCCTTCATTGACCTCAACTAC-3′, reverse, 5′-TCTCGCTCCTGGAAGATGG-3′.

2.6. Knockdown of endogenous MIZ-1 mRNA by siRNA

100 pmoles of siRNA against *MIZ-1* mRNA, synthesized in duplex and purchased from Bioneer (Daejeon, South Korea), were transfected into hDPSCs, using Lipofectamin RNAiMAX reagent (Invitrogen). Nucleotide sequences of siRNA against *MIZ-1* were: forward, 5′-GAAGGCCGAGAUCAGCAAA-3′, and reverse, 5′-UUUGCUGAUCUCGGCCUUC-3′.

2.7. Western blot analysis

Cells were harvested and lysed in radioimmunoprecipitation assay (RIPA) buffer. Cell extracts (30 μg) were separated by 12% SDS-PAGE, transferred onto ImmunBlot Polyvinylidene Difluoride (PVDF) membranes (BioRad, Hercules, CA, USA), and blocked with 5% skim milk (BD Biosciences, San Jose, CA, USA) or bovine serum albumin (Sigma-Aldrich). Membrane blots were incubated with antibodies against GAPDH or MIZ-1, followed by incubation with secondary antibodies conjugated to horseradish peroxidase (Vector Laboratories, Burlingame, CA, USA). Protein bands were visualized using an ECL kit (PerkinElmer, Waltham, MA, USA).

2.8. Oligonucleotide pull-down assays

Cells were lysed in HKMG buffer (10 mM HEPES, pH 7.9, 100 μm KCl, 5 mM $MgCl_2$, 10% glycerol, 0.1% NP-40, and 1 mM DTT), and the extracts incubated with 1 μg biotinylated double-stranded oligonucleotides for 16 h. Oligonucleotide probes were annealed by heating at 95 °C for 5 min in annealing buffer (100 μl of 1× TE +0.1 M NaCl), cooled slowly to room temperature, and pulled-down, as reported elsewhere [22]. Oligonucleotides sequences within the *Amelx* promoter

were as follows (only top strands are shown): *Amelx* promoter elements: MRE, 5′-TTTCATTCAGAAACCTGATTGGCTGTTCAA-3′. PCR-amplified products were used as templates for #1~#5 probe. The following oligonucleotides were used as PCR primers (only forward strand biotinylated): #1 forward, 5′-AGAAAGAACACCAGCGATTG-3′, reverse, 5′-GTCAAGTTTCTCCAGTGTAC-3′. #2 forward, 5′-CAAGAATGGGGATTCAATCC-3′, reverse, 5′-CATTGTCGACGT CTCAGT-3′. #3 forward, 5′-TTGCTAGAACTGAGACGTCG-3′, reverse, 5′-ATTAGTGCATATAGTCGTT-3′. #4 forward, 5′-CGACTATATGCACT AATCAC-3′, reverse, 5′-ATTTATATCATGCAGGGCAC-3′. #5 forward, 5′-CATGATATAAATTGGGGCAC-3′, reverse, 5′-ATGACCACAGT GGAGAT-3′.

2.9. Chromatin immunoprecipitation (ChIP)

Cells were fixed with formaldehyde (final 1%) to crosslink proteins to DNA. For detection of MIZ-1, protein-bound chromatin was immunoprecipitated with an anti-MIZ-1 antibody, as we have described previously [22]. An anti-immunoglobulin G (IgG) antibody was used as the ChIP negative control. PCR reactions were conducted using the following oligonucleotide primer sets, designed to amplify region of interest: the MRE of the *Amelx* promoter forward, 5′-AACACCAGCGATTGTGGAAT-3′, reverse, 5′- ATTTATATCA TGCAGGGCAC-3′.

2.10. Statistical analysis

Student's *t*-test was used for statistical analyses. P-values of < 0.05 were considered statistically significant.

3. Results and discussion

3.1. Differentiation of hDPSCs into odontoblasts and mRNA expression profiles of MIZ-1, AMELX and dentin-forming DSPP genes

DPSCs are mesenchymal stem cells (MSCs) present in the core region of the tooth pulp [23] that differentiate into odontoblast-like cells, pulpal fibroblasts, adipocytes, and neural-like cells [24]. hDPSCs

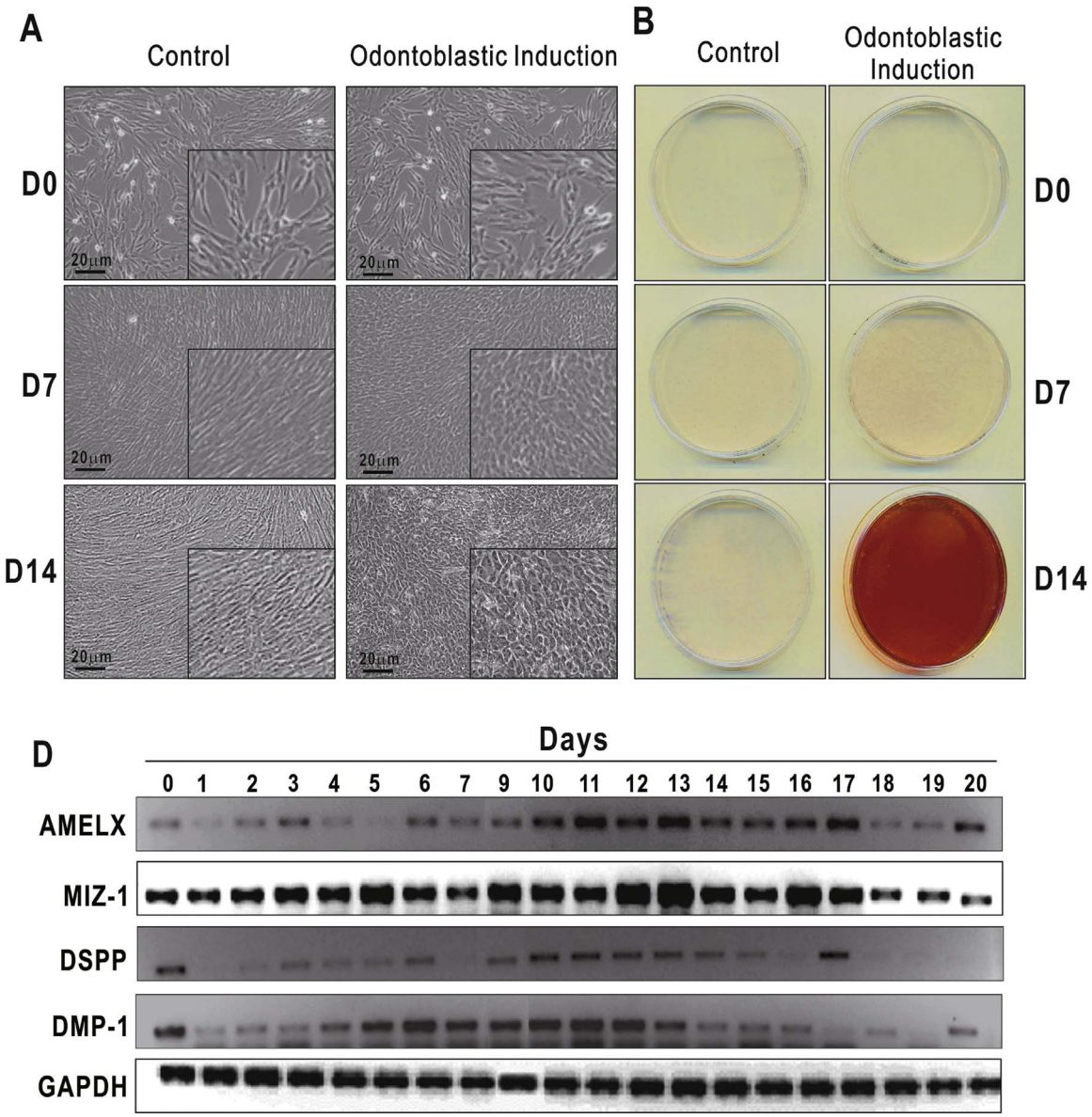

Fig. 1. Odontoblastic differentiation of hDPSCs mineralization, and mRNA expression profiles of *MIZ-1*, *AMELX*, *DSPP*, and *DMP-1* during odontoblastic differentiation. (A) Microscopic images of hDPSCs cultured with normal growth vs. odontoblasic induction media, for 0, 7, and 14 days. (B) Alizarin Red S staining of hDPSC mineralization at days 0, 7 and 14, post-induction. (C) mRNA expression profiles of *MIZ-1*, *AMELX*, *DSPP*, and *DMP-1* over 20 days of hDPSCs grown in odontoblastic differentiation medium..

abundantly express *AMELX* proteins during their differentiation into odontoblasts [17]. To test odontoblastic differentiation capability of hDPSCs, hDPSCs were cultured in induction medium for 14 days. Alizarin red staining was used to evaluate calcium-rich deposits in the cells cultured with normal medium or induction medium on days 0, 7, and 14 post-induction, exhibiting a flat, spindle-shape, and fibroblast-like morphology. At day 7, the hDPSCs cultured in normal growth medium were elongated in shape and continued to proliferate (Fig. 1A). However, hDPSCs grown in odontoblasic induction medium were polygonal in shape, with more dimensions, and showed only mild alizarin red staining, indicating an initiation of mineral deposition (Fig. 1A), which was markedly increased on 14d in differentiation medium (Fig. 1B). Using PCR, the mRNA expression profiles analyses of *MIZ-1*, *AMELX*, and the odontoblastic marker gene *DMP-1*, during odontoblastic differentiation of hDPSCs, showed that *AMELX* and *DMP-1* were temporally regulated in odontoblasic induction medium

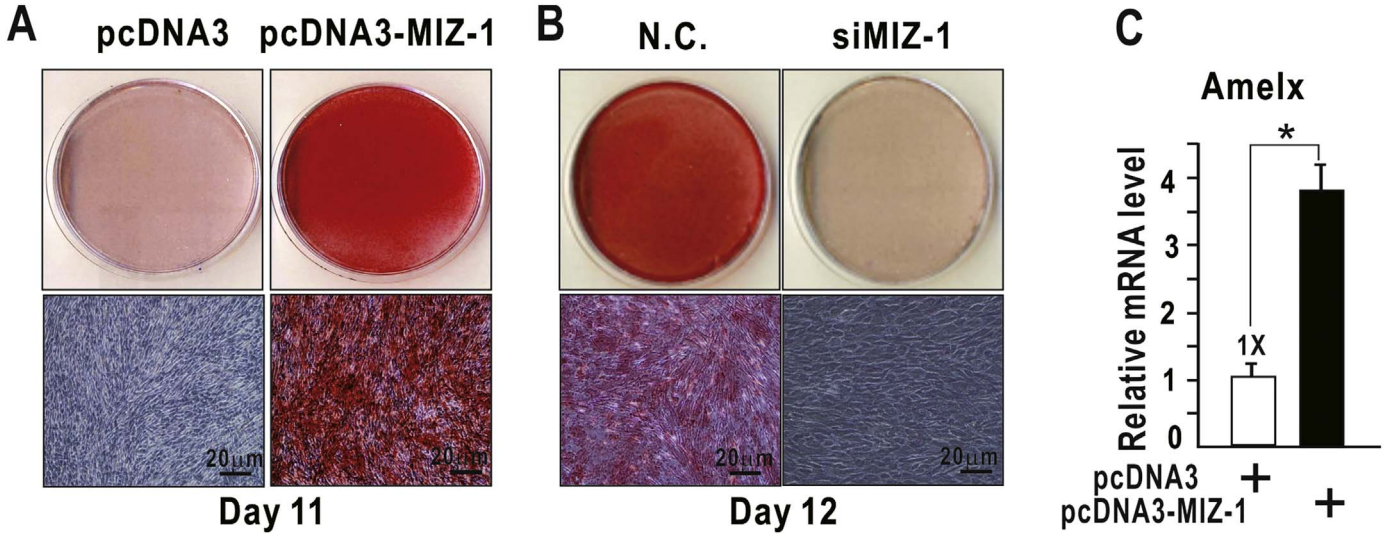

Fig. 2. MIZ-1 plays a pivotal role in mineralization of differentiated hDPSCs, and increases *Amelx* transcription levels. (A) Alizarin Red-S (AR-S) staining for mineralization of hDPSCs overexpressing MIZ-1. hDPSCs transfected with *MIZ-1* expression vector were cultured in odontoblastic induction medium for 11 days, and fixed and stained with AR-S. (B) AR-S staining of differentiated hDPSCs transfected with anti-*MIZ-1* siRNA. The cells were cultured in odontoblastic induction medium for 12 days, fixed, and stained with AR-S. (C) RT-qPCR analysis. MEF cells were transfected with a *MIZ-1* expression vector by electroporation, and endogenous *Amelx* mRNA measured by RT-qPCR at 48 h post transfection. mRNA levels were normalized to 18S ribosomal RNA..

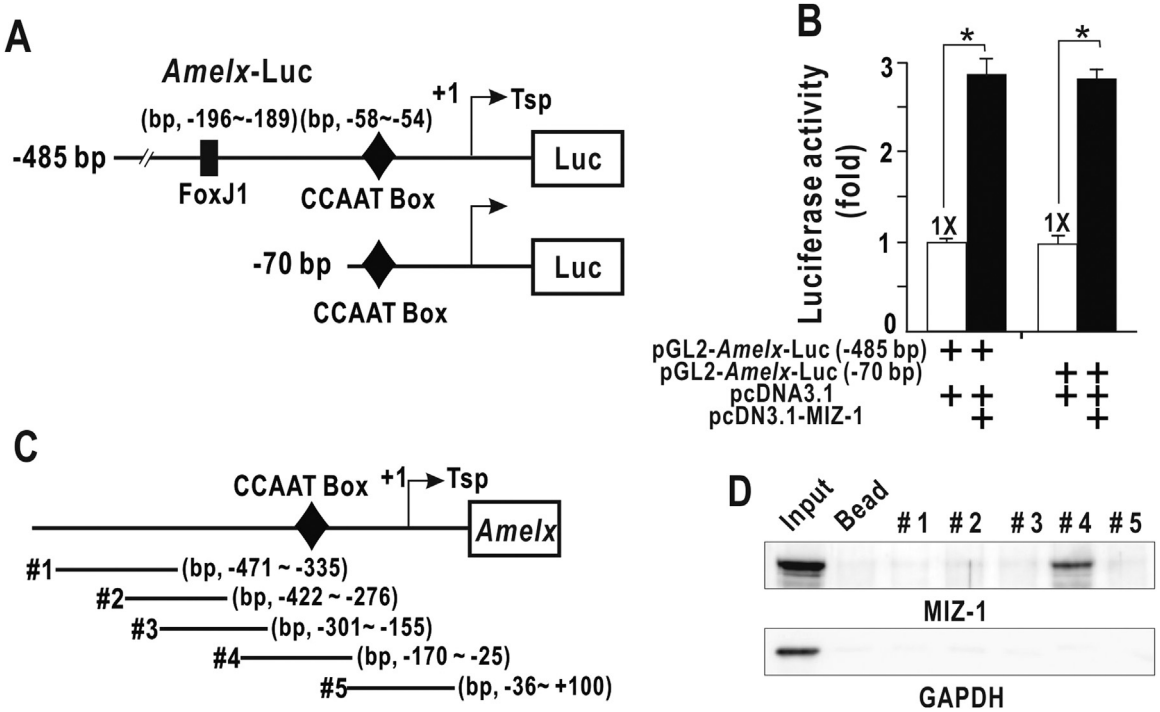

Fig. 3. MIZ-1 binds to an *Amelx* promoter MRE. (A) Diagram of the *Amelx* promoter–luciferase gene fusion reporter constructs tested. +1 (Tsp), transcription start point. ■, FoxJ1 binding site. (B) Transient transcription assays. The reporter plasmid and MIZ-1 expression vector were transiently transfected into LS8 cells and analyzed for luciferase activity 24 h after transfection, with normalization to co-expressed β-galactosidase activity. Data presented are the means of three independent assays. Error bars represent standard deviations. (C) Diagram of the *Amelx* promoter structure and location of five promoter regions tested for MIZ-1 binding., CAAT Box. (D) Oligonucleotide pull-down assays of MIZ-1 binding to five promoter elements within the *Amelx* promoter. Streptavidin agarose beads linked to biotinylated PCR products probes (#1 to #5) were incubated with LS8 cell lysates having ectopic *MIZ-1* expression. The precipitates were analyzed by western blot using an anti-MIZ-1 antibody.

(Fig. 1C). Interestingly, *MIZ-1* mRNA expression patterns were largely similar to those of the *AMELX* and *DSPP* genes (Fig. 1C).

3.2. MIZ-1 regulates mineralization in hDPSCs

Since the above data potentially suggested that MIZ-1 may regulate *AMELX* mRNA expression, and thereby, odontoblast differentiation and mineralization, we used a MIZ-1 gain vs. loss functional approach to examine this phenotype. hDPSCs were transfected with a *MIZ-1* expression vector or anti-*MIZ-1* siRNA. At day 11 after differentiation induction, hDPSCs cultured in odontoblast differentiation medium not only stained with alizarin red, but ectopic *MIZ-1* significantly increased mineral deposition, compared to control cells (Fig. 2A). At day 12, hDPSCs grown in odontoblast differentiation medium stained significantly by alizarin red, although *MIZ-1* knockdown decreased mineral deposition (Fig. 2B). These results suggested that MIZ-1 promotes differentiation of hDPSCs and mineralization. To further test whether MIZ-1 regulates *Amelx*, MEF cells were transfected with a *MIZ-1* expression vector (Fig. 2C), with RT-qPCR analysis showing that ectopic MIZ-1 increased endogenous *Amelx* gene expression, and thereby, mineralization of hDPSCs (Fig. 2C).

3.3. MIZ-1 regulates Amelx expression and binds to the Amelx gene promoter

Intrigued by the finding that MIZ-1 regulates transcription of *Amelx,* we next investigated possible mechanisms of such regulation. We prepared two different *Amelx* promoter reporter fusion constructs with long 5′ upstream (bp, −485 to +100) or short (bp, −70 to +100) promoter regulatory regions (Fig. 3A) [25,26]. These were then ligated into pGL2-Amelx-Luc reporter plasmids, and transfected into ameloblast-like LS8 cells, along with a full-length *MIZ-1* expression vector, showing that transcription of the two reporter constructs was activated similarly by MIZ-1 (Fig. 3B). To more distinctly identify the precise promoter regulatory region mediating transcriptional activation by MIZ-1, the *Amelx* promoter (bp, −485 to +100) was further divided into 5 regions partially overlapping with each other: #1 element (bp, −471 to −334), #2 element (bp, −422 to −276), #3 element (bp, −301 to −155), #4 element (bp, −170 to −25), and #5 element (bp, −36 to +100) (Fig. 3C). Oligonucleotide pull down assays using LS8 cell extracts showed that MIZ-1 strongly bound to the #4 element (bp, −170 to −25) (Fig. 3D). These results suggest that a sequence element located between bp, −70 to −25 of the *Amelx* promoter may be involved in transcriptional activation by MIZ-1.

3.4. MIZ-1 activates Amelx transcription via direct binding to the Amelx promoter MREs

We next analyzed the *Amelx* promoter nucleotide sequence for potential MIZ-1-binding element (MRE) using MacVector (Ver. 7.2) (Fig. 3A) [27]. One such element (bp, −70 to −49; 5′-TTCAGAAACCTGATTGG-3′), resembling the MIZ-1 binding consensus motif (5′-CCCACTCTCTGC-3′ or 5′-ATCGAT-3′), was identified, and oligonucleotide pull-down assays showed robust MIZ-1 binding (Fig. 3B). ChIP assays of MIZ-1 binding to the region flanking the MRE of the *Amelx* gene promoter further confirmed the DNA-protein

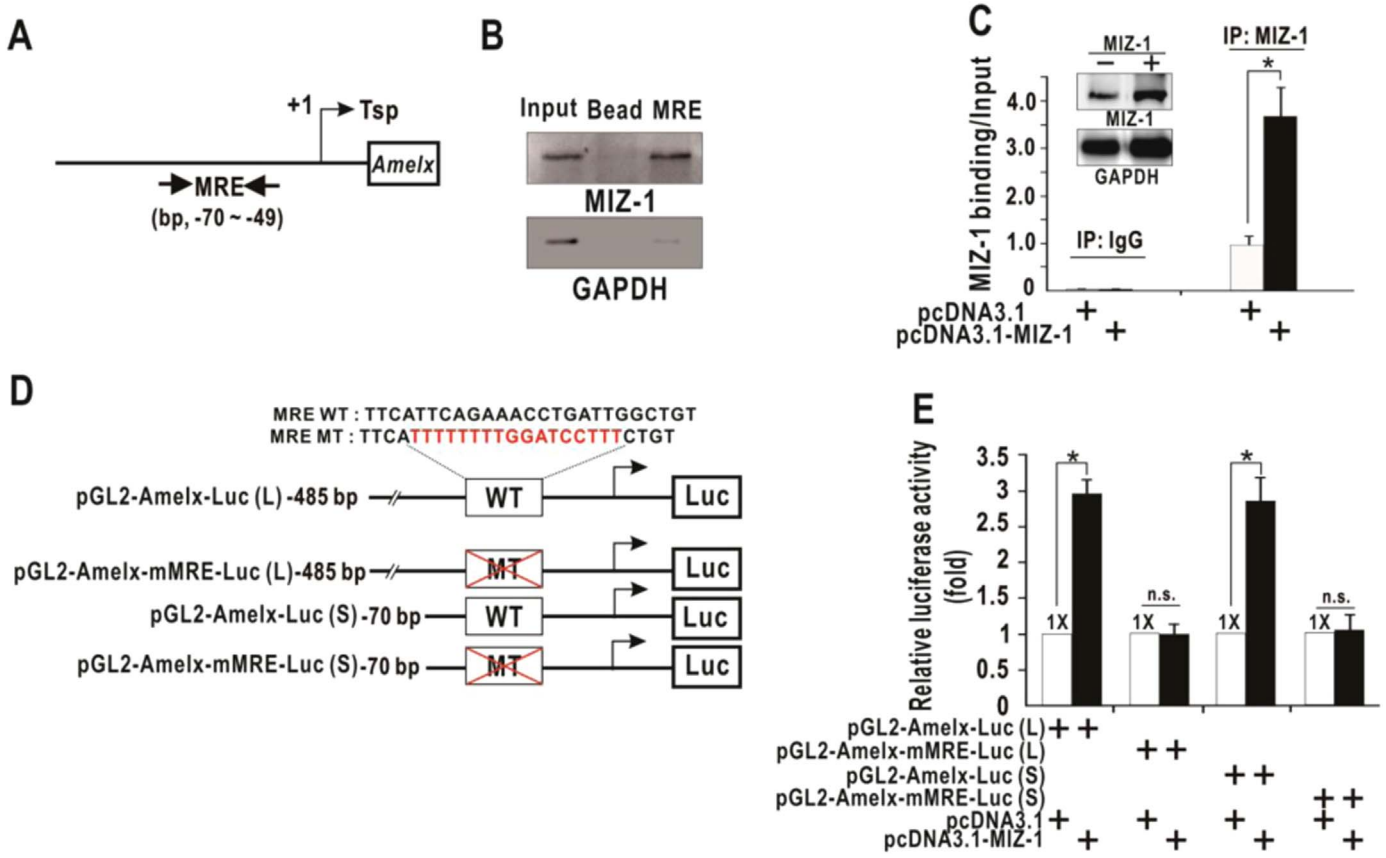

Fig. 4. MIZ-1 binds to an *Amelx* promoter MRE and induces transcription. (A) Diagram of the *Amelx* promoter structure. One MRE (MIZ-1 binding element) was found (bp, −70 to −49) using MacVector (ver. 7.2). (B) Oligonucleotide pull-down assays of the *Amelx* promoter MRE in LS8 cells. (C) ChIP-PCR assays of MIZ-1 binding to the MRE site located within the proximal *Amelx* promoter in LS8 cells. (D) Co-immunoprecipitation of MIZ-1, p300 and c-Myc. hDPSC cell lysates of mineralization at days 0 and 7 post-induction were immunoprecipitated using an anti-p300 and anti-c-Myc antibody, and analyzed by western blot using anti-MIZ-1 antibody. (E) Structures of the four luciferase gene fusion reporter constructs with or without MRE mutation. +1, (Tsp), transcription start point. (F) Transient transcription assays. Reporter plasmids and MIZ-1 expression vector were transiently cotransfected into LS8 cells and analyzed for luciferase activity 48 h later, with normalization to coexpressed β-galactosidase activity. Error bars represent standard deviations..

interaction in LS8 cells (Fig. 3C). Previous reports showed that MIZ-1 can bind to both p300 and c-Myc [28–30]. Although MIZ-1 interacts with p300 to activate transcription, its complexation with c-Myc represses transcription of target genes. Accordingly, we investigated changes in molecular interaction between MIZ-1 and p300, or c-Myc, during differentiation of hDPSC. hDPSC differentiation results in MIZ-1 upregulation, and c-Myc downregulation, and the interaction between MIZ-1 and p300 is significantly increased, while MIZ-1 interaction with c-Myc is little changed. The results suggested that transcription of Amelx promoter may be directly regulated by MIZ-1 binding (Fig. 4D). We further tested whether MIZ-1 could directly activate transcription of the *Amelx* promoter, by binding to the MRE element, using transient transfection and transcription assays in LS8 cells (Fig. 4E, F). We prepared two additional promoter and reporter gene fusion constructs, with mutations introduced into the MRE element by site-directed mutagenesis (5′-TTCAGAAACCTGATTGG-3′ was mutated to 5′-TTTTTTTTGGATCCTTT-3′) (Fig. 4E). Transient transfection assay of LS8 cells transfected with the reporter plasmid and a full-length MIZ-1 expression vector demonstrated that MIZ-1 activated transcription of the *Amelx* gene promoter constructs both with short and long promoter sequence similarly; MIZ-1, however, could not activate transcription of the two MRE-mutated constructs (Fig. 4F). These data suggest that MIZ-1 binds to the MRE and activates *Amelx* transcription.

In summary, we show that MIZ-1 is expressed during odontoblast differentiation activates transcription of Amelx by direct binding to the MRE of proximal promoter MRE. MIZ-1 is critical for odontogenesis and matrix mineralization during tooth development.

Acknowledgments

This work was primarily supported by a DOYAK Research Grant (2011-0028817); Medical Research Center Grant (2011-0030086 to M.-W.H.) from the National Research Foundation (NRF) of the Korean Ministry of Education, Science and Technology.

Transparency document A. Supporting information

Supplementary data associated with this article can be found in the online version at http://dx.doi.org/10.1016/j.bbrep.2016.10.007.

References

[1] I. Thesleff, P. Sharpe, Signalling networks regulating dental development, Mech. Dev. 67 (1997) 111–123.
[2] I. Thesleff, M. Mikkola, The role of growth factors in tooth development, Int. Rev. Cytol. 217 (2002) 93–135.
[3] I. Thesleff, Epithelial-mesenchymal signalling regulating tooth morphogenesis, J. Cell Sci. 116 (2003) 1647–1648.
[4] A.G. Fincham, J. Moradian-Oldak, J.P. Simmer, The structural biology of the developing dental enamel matrix, J. Struct. Biol. 126 (1999) 270–299.
[5] J.D. Termine, A.B. Belcourt, P.J. Christner, K.M. Conn, M.U. Nylen, Properties of dissociatively extracted fetal tooth matrix proteins. I. Principal molecular species in developing bovine enamel, J. Biol. Chem. 255 (1980) 9760–9768.
[6] C.E. Smith, Cellular and chemical events during enamel maturation, Crit. Rev. Oral. Biol. Med. 9 (1998) 128–161.
[7] M. Lagerstrom, N. Dahl, Y. Nakahori, et al., A deletion in the amelogenin gene (AMG) causes X-linked amelogenesis imperfecta (AIHl), Genomics 10 (1991) 971–975.
[8] M.J. Aldred, P.J. Crawford, E. Roberts, N.S. Thomas, Identification or a nonsense mutation in the amelogenin gene (AMELX) in a family with X-linkcd amelogenesis imperfecta (AIHI), Hum. Genet. 90 (1992) 413–416.
[9] N.J. Lench, A.H. Brook, G.B. Winter, SSCP detection of a nonsense mutation in exon 5 of the amelogenin gene (AMGX) causing X-linked amelogenesis imperfecta (AIH1), Hum. Mol. Genet. 3 (1994) 827–828.
[10] R.I. Couwenhoven, S.A. Schwartz, M.L. Snead, Arrest of amelogenin transcriptional activation in bromodeoxyuridine-treated developing mouse molars in vitro, J. Craniofac Genet. Dev. Biol. 13 (1993) 259–269.
[11] M.L. Snead, M.L. Paine, L.S. Chen, et al., The murine amelogenin promoter: developmentally regulated expression in transgenic animals, Connect. Tissue Res. 35 (1996) 41–47.
[12] T.G. Diekwisch, J. Ware, A.G. Fincham, M. Zeichner-David, Immunohistochemical similarities and differences between amelogenin and tuftelin gene products during tooth development, J. Histochem. Cytochem. 45 (1997) 859–866.
[13] M. Zeichner-David, H. Vo, H. Tan, et al., Timing of the expression of enamel gene products during mouse tooth development, Int. J. Dev. Biol. 41 (1997) 27–38.
[14] J. Jacques, D. Hotton, M. De la Dure-Molla, et al., Tracking endogenous amelogenin and ameloblastin in vivo, PLoS One 9 (2014) e99626.
[15] S.R. Venugopalan, X. Li, M.A. Amen, S. Florez, et al., Hierarchical interactions of homeodomain and forkhead transcription factors in regulating odontogenic gene expression, J. Biol. Chem. 286 (2011) 21372–21383.
[16] A. Veis, The chemistry and Biology of Mineralized Tissues, EBSCO Media, 1985, pp. 170–184.
[17] W.T. Butler, Dentin matrix proteins and dentinogenesis, Connect Tissue Res. 33 (1995) 59–65.
[18] A. Linde, M. Goldberg, Dentinogenesis, Crit. Rev. Oral. Biol. Med. 4 (1993) 679–728.
[19] O. Albagli, P. Dhordain, C. Deweindt, G. Lecocq, D. Leprince, The BTB/POZ domain: a new protein-protein interaction motif common to DNA- and actin-binding proteins, Cell Growth Diff. 6 (1995) 1193–1198.
[20] J.A. Costoya, Functional analysis of the role of POK transcriptional repressors, Brief. Funct. Genom. Prote. 6 (2007) 8–18.
[21] K.F. Kelly, J.M. Daniel, POZ for effect–POZ-ZF transcription factors in cancer and development, Trends Cell Biol. 16 (2006) 578–587.
[22] D.I. Koh, D. Han, H. Ryu, W.I. Choi, B.N. Jeon, M.K. Kim, KAISO, a critical regulator of p53-mediated transcription of CDKN1A and apoptotic genes, Proc. Natl. Acad. Sci. USA 21 (2014) 15078–15083.
[23] T. Kaori, N. Takako, S. Eriko, et al., Stage-specific functions of leukemia/lymphoma-related actor (LRF) in the transcriptional control of osteoclast development, Proc. Natl. Acad. Sci. USA 109 (2012) 2561–2566.
[24] H. Kim, D. Dejsuphong, G. Adelmant, et al., Transcriptional repressor ZBTB1 promotes chromatin remodeling and translesion DNA synthesis, Mol. Cell. 54 (2014) 107–118.
[25] Y.L. Zhou, M.L. Snead, Identification of CCAAT/enhancer-binding protein alpha as a transactivator of the mouse amelogenin gene, J. Biol. Chem. 275 (2000) 12273–12280.
[26] S.R. Venugopalan, X. Li, M.A. Amen, et al., Hierarchical interactions of homeodomain and forkhead transcription factors in regulating odontogenic gene expression, J. Biol. Chem. 286 (2011) 21372–21383.
[27] B.L. Barrilleaux, D. Burow, S.H. Lockwood, A. Yu, D.J. Segal, P.S. Knoepfler, Miz-1 activates gene expression via a novel consensus DNA binding motif, PLoS One 9 (2014) e101151.
[28] S. Wu, C. Cetinkaya, M.J. Munoz-Alonso, N. von der Lehr, F. Bahram, V. Beuger, et al., Myc represses differentiation-induced p21CIP1 expression via Miz-1-dependent interaction with the p21 core promoter, Oncogene 23 (2003) 351–360.
[29] A.L. Gartel, K. Shchors K, Mechanisms of c-myc-mediated transcriptional repression of growth arrest genes, Exp. Cell Res. 283 (2003) 17–21.
[30] P. Staller, K. Peukert, A. Kiermaier, et al., Repression of p15INK4b expression by Myc through association with Miz-1, Nat. Cell Biol. 3 (2001) 392–399.